minerals

MDPI

Article

Proposal for an Environmentally Sustainable Beneficiation Route for the Amphibolitic Itabirite from the Quadrilátero Ferrífero-Brazil

Gizele Maria Campos Gonçalves [1] and Rosa Malena Fernandes Lima [2,*]

[1] Mine Planning at Brucutu Mine—Vale, São Gonçalo do Rio Abaixo, Rio de Janeiro CEP 35.935-000, Brazil; gizele.campos@vale.com

[2] Mining Engineering Department, School of Mines, Federal University of Ouro Preto, Ouro Preto 35400-000, Brazil

* Correspondence: rosa@ufop.edu.br

Received: 27 July 2020; Accepted: 4 October 2020; Published: 10 October 2020

Abstract: The high world demand for iron ores opposed to the rapid exhaustion of high-grade deposits from the main producing regions around the world has motivated the search and/or improvement of beneficiation routes, which enable the economic use of iron formations previously considered marginal ores, which have the potential to considerably increase mineable reserves due to their large volume. In this study, a sample of amphibolitic itabirite from the eastern region of the Quadrilátero Ferrífero, minas Gerais, Brazil was characterized, aiming at its use in the industrial pelletizing circuit. The main physical characteristics of this ore are moisture = 10% and specific weight = 3710 kg/m^3. The ore has a high grade of loss on ignition—LOI (6.7%) and P (0.14%). Through X-ray diffractometry (XRD), optical microscopy and scanning electron microscope—SEM, the ore was found to consist of 64.5% goethite (amphibolitic, alveolar, massive and earthy); 6.8% hematite (martitic, granular and lamellar) and 0.9% magnetite. The main gangue mineral is quartz (25.5%). Based on the results of concentration tests (magnetic and flotation) performed with the studied sample, the magnetic concentration route of deslimed sample followed by the addition of slimes in magnetic concentrate can be incorporated into the pelletizing process.

Keywords: amphibolitic itabirite; goethite; iron ore; magnetic concentration; flotation

1. Introduction

Iron ore is the second-most traded mineral commodity on the market, mainly for the manufacture of cast iron and steel (98% of the world production) [1–3]. It corresponds to 15% of the products exported by Brazil, which stands as the third-largest iron-producing country and holds 12% of the world reserves, located mainly in the provinces of Quadrilátero Ferrífero, minas Gerais (MG) and Carajás, Pará (PA) [4,5].

The exhaustion of high-grade iron ore deposits from the main producing regions, located in Brazil, Australia, India and others, coupled with increased demand in the world market and increasingly severe environmental restrictions, have imposed a great challenge for the mineral industry. This current situation implies the development of beneficiation routes for marginal ores, aiming at greater metallic recovery and the minimization of tailings disposal, as well as the reprocessing of tailings deposited in dams, with Fe grades greater than 30%, to obtain products within the specifications for the steel industry [6,7].

Mineralogical compositions of slimes from desliming operations of industrial flotation circuits of Brazilian iron ores have a high proportion of goethite (in some cases, >50%), followed by martitic hematite; quartz and smaller proportions of magnetite, kaolinite and gibbsite. The Fe

grades of this material are between 30–53%. Silva and Luz [8] carried out the magnetic concentration of a slime thickener underflow sample (100% −150 μm, with grades of 32.9% Fe, 37.7% SiO_2, 5.3% Al_2O_3 and 5.7% loss on ignition—LOI)) from a mine located in Quadrilátero Ferrífero. The magnetic field intensities tested were of 0.6, 0.9 and 1.2 T. The best result after a cleaner step was obtained with a magnetic field of 1.2 T: 64.6% Fe, 5.5% SiO_2 and a mass recovery of 62.8%. For an underflow sample of slime thickener from the Brucutu mine (46% Fe, 15% SiO_2, 10% Al_2O_3 and 10% LOI), there was obtained a concentrate with 66.8% Fe, 0.8% SiO_2, 0.97% Al_2O_3 and 2.4% LOI for a magnetic field of 1.45 T. however, the mass recovery was very small (12.7%), due to the fine size distribution of the sample (d_{80} = 10 μm) [9].

Different processes of metamorphism and weathering of iron formations in the different geographical regions of Quadrilátero Ferrífero led to the formation of different typologies of ores, which are classified as compact, semi-compact and friable itabirites, according to the percentage retained in a given mesh. The grades of Fe in these ores vary between 30% and 60%. At the western edge of Quadrilátero Ferrífero, compact itabirites comprise a percentage retained >55% +6.3 mm, semi-compact (between 30% to 55% +6.3 mm) and friable (<30% +6.3 mm) [10]. At the central and eastern portions, there are a predominance of friable ores, and among them, there are the amphibolitic (~1.2% Al_2O_3, p > 0.14% and LOI > 5%) and aluminous itabirites (Al_2O_3 > 3.0% and LOI > 3%) of Alegria's (60% −0.15 mm) and Brucutu's (80% −8 mm) deposits [11,12]. These ores have a high proportion of goethite, generating large amounts of slimes, which cause problems both in the concentration by flotation and in the dewatering stages (thickening and filtration). For this reason, they are considered marginal or, depending on their grade, they are used as a natural fine sinter feed [11–13].

In this study, a characterization (physical, chemical and mineralogical) was carried out on a sample of amphibolitic itabirite (marginal ore) from the eastern region of the Quadrilátero Ferrífero, which corresponds to 15% of the current reserves (263 million tons) of Brucutu [13], aiming at the development of an adequate processing route to obtain a concentrate of this typology of ore to be incorporated into the industrial pelletizing process.

2. Materials and Methods

The amphibolitic itabirite sample used in this study was obtained by the composition of two subsamples: A1 (28 kg, 55.8% Fe) and A2 (52 kg and 41.2% Fe). These were collected in two different regions of amphibolitic itabirite in Brucutu's deposit (Figure 1), aiming at obtaining a Fe grade (~46%), compatible with ore grades current feed in industrial concentration plants in Quadrilátero Ferrífero [6,11,14], since the friable ores with grades higher than 50% Fe can be used as a natural fine sinter product [13]. As seen in Figure 1, the ore has an ocher color and a clay appearance.

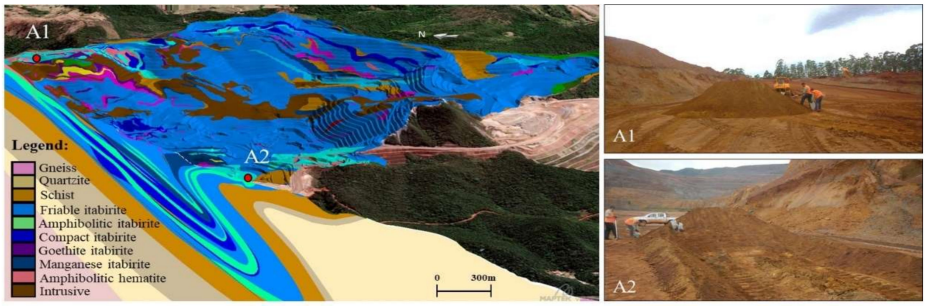

Figure 1. Geological section and map of Brucutu's deposit, with the location of the two regions where the subsamples A1 and A2 (right side) of the amphibolitic itabirite were collected.

After the homogenization of the amphibolitic itabirite sample ROM (run of mine), aliquots were removed for physical characterization: moisture determination, specific weight and size distribution; chemical: determination of Fe_{Total}, SiO_2, Al_2O_3, CaO, MgO, MnO, Fe_3O_4, P and LOI grades and mineralogical: mineral phases identification and determination of the quartz's liberation.

After determining the ore's liberation mesh, a part of the sample was comminuted at −105 μm for exploratory concentration tests.

2.1. Physical Characterization

The natural moisture (wet basis) of the ore sample was performed in a furnace at 100 °C (±5). The specific weight (average of the values obtained by 3 scans) was determined by the Quantachrome Corporation pycnometer Ultrapyc 1200e/UPY-30 model (Boynton Beach, FL, USA) in accordance with the methodology of Silva et al [3].

The determination of the ore's size distribution, carried out in duplicate, was achieved through wet sieving (sieves from 8000 to 45 μm) and a laser particle size analyzer (fraction −45 μm), CILAS 1180 model, used under the following conditions: 60 s of ultrasound, 25% obscuration and the addition of 10 drops of sodium hexametaphosphate at 1% *w*/*v* to disperse the suspension.

2.2. Chemical Characterization and Loss on Ignition (LOI)

The ROM sample's grades of Fe_{Total}, SiO_2, P, Al_2O_3, MnO, MgO, TiO_2 and CaO, by size fraction, as well as the concentration tests products, were determined by X-ray fluorescence—XRF (Rigaku X-ray spectrometer Simultix 14 model, Rigaku, Osaka, Japan). For this, fused pellets were made at 1000 °C of a mixture consisting of 1 g of each pulverized sample (−38 μm) and 5 g of lithium tetraborate/metaborate (67% $Li_2B_4O_7$/33% $LiBO_2$). The Fe_3O_4 grade (1.3 g samples) was determined by Rapiscan's Satmagan 135 equipment (Rapiscan, Skudai—Johor, Malaysia) according to the methodology described by Breuil et al. [15] and Stradling [16].

The experimental procedure for determining the loss on ignition (LOI) consisted of introducing the sample (150 g) in a muffle furnace, regulated at a temperature of 1000 °C, where it remained for 1 h, and the loss on ignition calculation was determined by the percentage of sample mass loss after calcination in relation to the initial mass.

2.3. Mineralogical Characterization

X-ray diffractometry—XRD (total powder method) was used to identify the mineral phases of the studied sample. For this, a PaNalytical model X'pert^{3}Powder diffractometer (Malvern Instruments, Malvern, UK) equipped with a Cu tube (λ_{Cu} = 1.5405 Å) and Ni filter was used. The operation conditions were: 45 kV and current of 40 mA and scanning angle (2θ) from 5° to 90° counting time of 15 min. The data were collected by using the X-ray Data Collector software (version 5.4). mineral phases identification in the X-ray diffraction pattern was performed by the software highScore Plus (version 4.5), using the standard database X-ray patterns of the ICCD PDF-2, 2015.

Thermogravimetric analysis was used to confirm/identify the hydrated mineral phases present in the sample. The experimental procedure consisted of the introduction of a platinum crucible, containing the sample in the TA Instruments model TGA Q50 thermogravimetric analyzer (New Castle, DE, USA). Data collection was performed by the TA Instruments Explorer software (version 4.5A) under the following conditions: heating from 20 to 1000 °C, heating rate of 10 °C/min, isotherm of 5 min at 1000 °C and N_2 flowrate = 100 mL/min (10 mL/min for cooling the thermobalance and 90 mL/min for purging the sample).

For textural studies of the amphibolitic itabirite, performed by optical microscopy (Leica optical microscope—DMLP) (Leica, Werzlar, Germany) and scanning electron microscopy (Hitachi SU3500 Tokyo, Japan) SEM, polished sections were made by inlaying 3 g of sample with a mixture of epoxy resin and the respective catalyst from the Epoxiglass brand (2:1 ratio). Afterwards, they were lapped (sandpaper: 180, 220, 320, 400, 600 and 800) and polished (diamond pastes of 6 μm, 3 μm, 1 μm and 1/4 μm). The determination of the quartz's liberation in regard to the iron minerals was performed by optical microscopy (Gaudin's method) by counting 200 particles in each size fraction.

2.4. Magnetic Concentration and Flotation Tests

The preparation of the sample studied for the concentration tests (magnetic and flotation) consisted of ROM classification/fragmentation in particle size −105 μm. For this, at first, the ROM was classified by wet sieving at −105 μm. After drying, only the fraction size +105 μm (79 kg) was dry-grinded by a laboratory rod mill for 1 min, followed by wet sieving −105 μm so as not to generate excessive slimes (−10 μm particles). This procedure was done until all sample reached −105 μm particle size. Finally, the prepared sample was dried, homogenized and splited into subsamples to perform the tests with non-deslimed and deslimed ore. For the desliming operation, 20 L of pulp with 25 wt% solids at pH 10.5 (adjusted with NaOH solution at 50% *w*/*v*) was stirred at 1200 rpm for 5 min. Then, the pulp was allowed to stand for 13 min to settle the 10 μm particles, and the supernatant (−10 μm particles) was removed. The initial volume was completed again, and this procedure was repeated 3 more times.

For magnetic concentration tests carried out with a non-deslimed sample, a magnetic carrousel concentrator (Minimag, Gaustec, Nova Lima, Brazil) with a 1.5 mm matrix gap was used. First, the equipment was switched on. Then, the magnetic field intensity was adjusted to the desired value (0.9 or 1.1 T), and the water tap was opened at 1 kgf/cm^2 pressure. After, the magnetic field's stabilization (20 min), the feed (rate of 5.7 kg/h) was continually fed in a closed circuit into the equipment. After the sample feeding finished, the flow of the feed and products magnetic and non-magnetic were simultaneously sampled. Then, they were filtered, dried, weighted and pulverized for chemical analysis in order to perform the mass and metallurgical balances. For the deslimed sample, the INBRAS L4 model magnetic concentrator with a 2.5 mm gap matrix was used. Firstly, the equipment was switched on, and the magnetic field was adjusted to 0.9 T (coil current of 15 A). After the magnetic field's stabilization time (10 min), the washing water tap was opened at a flow rate of 20 mL/s, and the aliquot of the deslimed sample (25 g) was slowly added to the equipment's feeder. After separation, the container holding the waste was removed. Another container was then inserted, the equipment turned off and the concentrate removed. This procedure was repeated 5 times. Finally, the magnetic separation products were filtered, dried and weighed, followed by homogenization, quartering and pulverization for chemical analysis of the products, which were later used in mass and metallurgical balances.

Reverse cationic flotation tests were carried out only with the deslimed sample under the following conditions: pH 10.5, pulp with 50 wt% solid and 500 g/ton of starch and amine with 50% neutralization degree (Flotigam 7100-Clariant): 170 and 200 g/ton. After adding the sample and water inside the flotation cell CDC—CFB 1000 EEPNBA model (1.2 L volume), the cell speed was adjusted to 1200 rpm, then gelatinized corn starch with NaOH was added and conditioned for 3 minutes, followed by the addition of amine, and conditioned for 1 min more. Finally, the air tap was opened, and flotation was carried out until the froth exhaustion. The float (tailing) and sunk (concentrate) products were filtered, dried and weighed, followed by homogenization, quartering and pulverization for chemical analysis, which were later used in mass and metallurgical balances.

3. Results and Discussion

3.1. Physical Characterization

The average value of moisture (wet basis) of the amphibolitic itabirite sample was 10% (standard deviation of 0.5), which is consistent with the moisture values of hydrated ores in Quadrilátero Ferrífero (6% to 10%), attributed to the presence of porous goethite and martitic hematite varieties, which retain moisture due to the high porosity of these minerals [11,13,14]. The specific weight was 3710 kg/m^3 (standard deviation of 0.15), which is also consistent with the values of the specific weights of friable ores in the eastern region of Quadrilátero Ferrífero (2600 to 3930 kg/m^3), since the ores in this region are quite porous [11,17].

Figure 2 shows the particle size distribution curves of the amphibolitic itabirite samples studied: ROM, −105 μm, −105 μm deslimed and slimes.

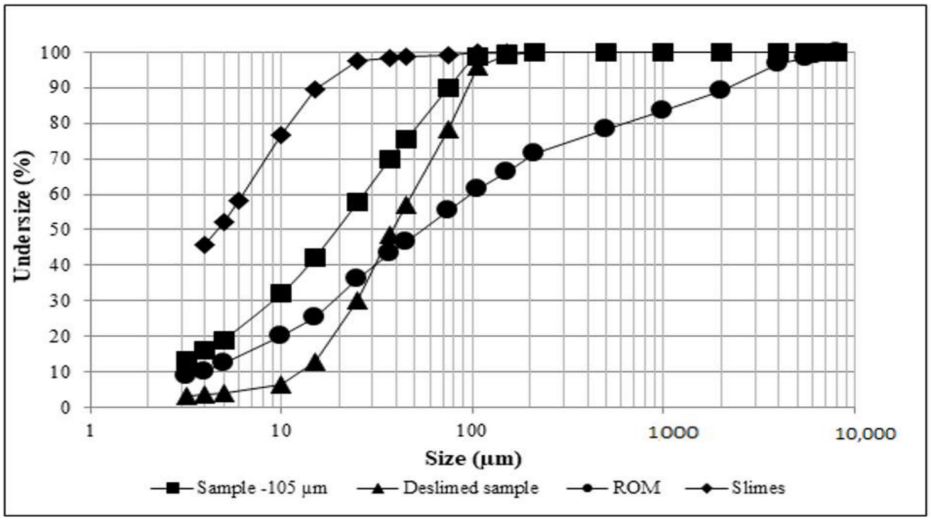

Figure 2. Size distribution curves of the amphibolitic itabirite samples studied: run of mine (ROM), −105 µm, deslimed and slimes.

As can be seen from the ROM's particle size distribution curve, the amphibolitic ore studied can be classified as friable, since the +6300 µm fraction is less than 10%, 80% −8000 µm and 60% −150 µm [10–13]. The d_{80} of the ROM sample, −105 µm sample and deslimed sample were of 800, ~50 and ~80 µm, respectively. When comparing the particle size distribution curves, an increase of 10% in slimes was noticeable after the ROM sample was comminuted to −105 µm; however, there was a removal of 23% of slimes when the comminuted sample was deslimed (see Figure 2). The increase in the proportion of slimes generated in the comminuted product is related to the presence of goethite and martitic hematite varieties, which are very common in this type of ore [3,11,17–19]. The d_{80} of the slimes was approximately 10 µm, owing the removal of −10 µm particles in the desliming step. This operation is essential, because the slimes are problematic for the subsequent concentration and dewatering steps.

3.2. Chemical Characterization

Table 1 shows the chemical composition and loss on ignition (LOI) by size fraction of the ROM sample of amphibolitic itabirite.

Table 1. Chemical composition and loss on ignition (LOI) by size fraction of the run of mine (ROM) of the amphibolitic itabirite sample.

Size Fraction (µm)	Weight (%)	Grade (%)										Distribution (%)			
		Fe_{Total}	Fe_3O_4	SiO_2	P	Al_2O_3	Mn	CaO	MgO	TiO_2	LOI	Fe	SiO_2	P	LOI
+1000	17.80	41.50	0.26	31.55	0.14	0.82	0.20	0.02	0.19	0.02	5.62	16.0	22.0	17.9	14.9
−1000 +500	4.90	45.10	0.78	27.09	0.15	0.88	0.41	0.02	0.16	0.04	6.66	4.8	5.2	5.3	4.9
−500 +150	13.50	47.90	1.20	26.90	0.10	0.67	0.20	0.01	0.09	0.06	4.32	14.0	14.2	9.7	8.8
−150 +45	21.70	37.80	1.10	40.93	0.08	0.49	0.08	0.02	0.08	0.04	3.98	17.8	34.8	12.5	12.9
−45	42.20	51.70	0.99	14.32	0.18	1.34	0.13	0.02	0.17	0.07	9.28	47.3	23.7	54.6	58.5
Total	100.0	46.04	0.90	25.47	0.14	0.95	0.15	0.02	0.14	0.05	6.69	100.0	100.0	100.0	100.0

As can be seen in Table 1, the studied amphibolitic itabirite is a hydrated ore with LOI above 5%. Fe_{Total}, P, Al_2O_3 and LOI grades are higher in the size fraction −45 µm. The inverse occurs with SiO_2. Therefore, for the use of this ore, it is necessary to introduce a concentration process. The grades of Fe_3O_4 determined correspond exactly to the proportion of magnetite present in the ore, which is a low value. Thus, it will not be necessary to use a low-intensity magnetic separation (<0.2 T) for

prior removal of the magnetite before the medium-intensity magnetic separation and high-intensity magnetic concentration (>0.2 T) [20].

3.3. Mineralogical Characterization

Figures 3 and 4 present an X-ray diffraction pattern and thermogram of the ROM sample (fraction size −45 μm), respectively.

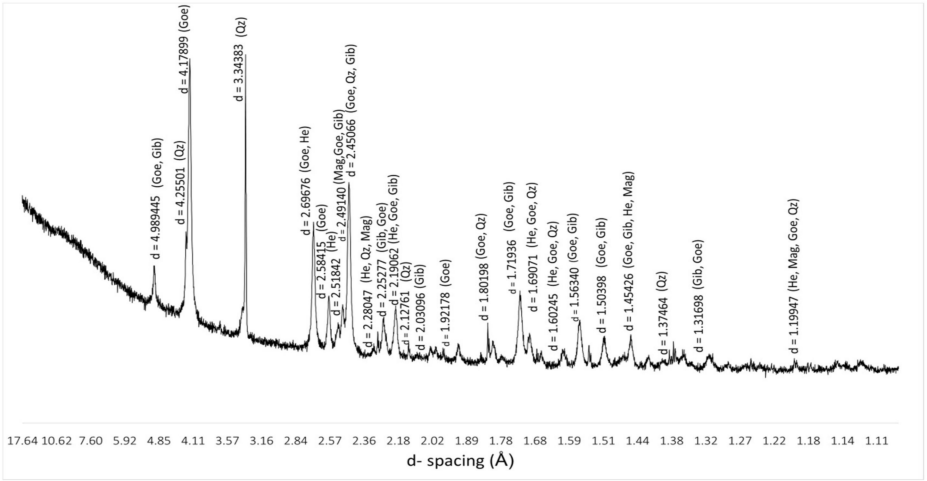

Figure 3. X-ray diffraction pattern of the size fraction −45 μm of the amphibolitic itabirite (ROM).

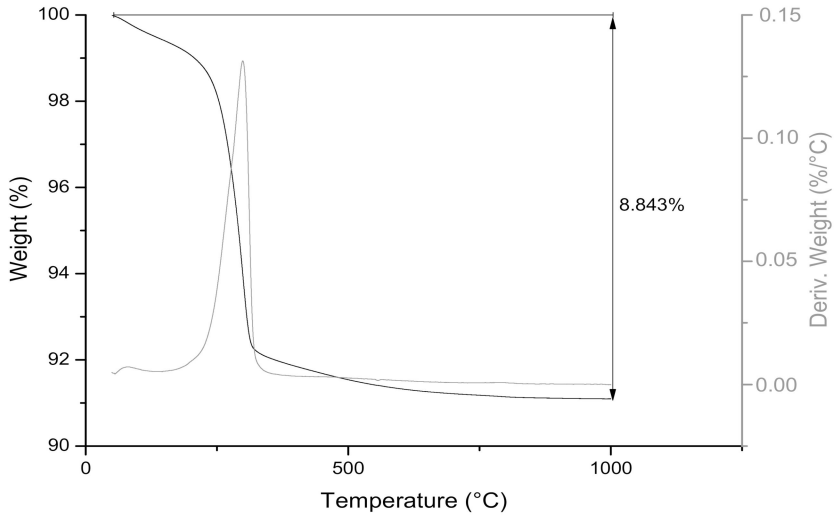

Figure 4. Thermogram of the size fraction −45 μm of the amphibolitic itabirite (ROM).

Table 2 presents the d-spacing of the PDF-2 X-ray diffraction pattern references, which were used to identify the minerals goethite, hematite, magnetite, quartz and gibbsite in the X-ray diffraction pattern of Figure 3. Table 3 presents the estimative of the mineralogical composition of the ROM and, consequentially, of the non-deslimed −105 μm sample, which was determined by stoichiometric calculus, taking into account the chemical composition of ROM from Table 1 and the theoretical chemical formula of the identified minerals (Table 2). For this, the grade of Al_2O_3 was assumed to belong only to gibbsite. For this reason, besides the low grade of Al_2O_3 (0.95 wt%), the gibbsite content in the sample probably was overestimated, once it was well-known that Al can substitute Fe in the crystalline structure of goethite, as reported in the literature [21]. In addition, the hematite content can be underestimated. As can be seen, the proportion of goethite is very high (64.5 wt%). The opposite is observed with quartz (25.5 wt%) and hematite (6.8 wt%) contents. Based on the mineralogical

composition of the studied sample, the magnetic concentration of medium-to-high field is the most suitable concentration method for this type of ore [6–9].

Table 2. X-ray diffraction patterns reference PDF 2 used to identify the minerals in the diffraction pattern of the size fraction −45 μm of the amphibolitic itabirite (ROM).

PDF-2 Ref. Code	Mineral	d-spacing (Å)
96-901-6407	Goethite (Goe)	4.98000; **4.17986;** 2.69307; 2.58415; 2.49000; 2.44951; 2.24334; 2.19031; 1.92196; 1.80149; 1.77368; 1.71910; 1.69052; 1.66000; 1.60380; 1.56442; 1.51150; 1.45506; 1.42142; 1.37989; 1.36866; 1.35592; 1.31809; 1.19941; 1.15119; 1.12679
96-591-0083	hematite (He)	**2.68150;** 2.50400; 2.27450; 2.19363; 1.83013; 1.68362; 1.59390; 1.44569; 1.19824
96-900-2327	Magnetite (Mag)	**2.47661;** 1.45204; 1.19824; 1.15019; 2.12739; 2.02866; 1.77653; 1.71492; 1.68179; 1.65838; 1.60134; 1.56167;
96-901-3322	Quartz (Qz)	4.25478; **3.34321;** 2.45650; 2.28123; 1.81777; 1.80167; 1.65906; 1.45281; 1.38198; 1.37487; 1.19771
96-101-1082	Gibbsite (Gb)	**4,84454;** 4,30676; 2.69498; 2.49837; 2.46084; 2.18702; 1.68179; 1.65838; 1.60134; 1.53953; 1.50229; 1.45643; 1.38128; 1.31527

Bold form: d-spacing of highest intensity peak.

Table 3. Mineralogical composition of the amphibolitic itabirite (ROM).

Mineral	Chemical Formula	Weight (%)
Goethite	FeO·OH	64.5
Quartz	SiO_2	25.5
Hematite	Fe_2O_3	6.8
Gibbsite	$Al(OH)_3$	1.1
Magnetite	Fe_3O_4	0.9
Others	-	1.2

As can be observed in the thermogram (Figure 4) is the first region of weight loss up 200 °C due to the loss of physically adsorbed water by the van der Walls bond (environment temperature), which is removed by air purging of the sample and hydrogen bonds on goethite [21–27]. The highest weight loss from 200–310 °C is due to the dehydroxylation of goethite to hematite ($2FeO{\cdot}OH \rightarrow Fe_2O_3{\cdot}H_2O$) [22–27]. however, the dehydroxylation of gibbsite only occurs in one step at 295 °C [28]. Therefore, the thermogram of the −45 μm size fraction of ROM is coherent with the identified minerals in the X-ray diffraction pattern (see Figure 3).

Figure 5 shows optical microscopy images of the size fractions +1000 μm (a), −1000 +500 μm (b), −500 +150 μm (c) and −150 +45 μm.

Figure 5a shows the presence of porosity in the alveolar goethite and mainly in the amphibolitic (top-right grain). Quartz grains occur associated (mixed) with alveolar (left corner) and massive (central portion) goethite particles. Figure 5b shows a mixed particle in the central part (quartz with goethite and martitic hematite), showing the process of martitization of magnetite (central region of the grain) to hematite (grain edges). In the lower left part, a mixed particle consisting of alveolar goethite, quite porous, quartz and amphibolitic goethite is observed, which is also observed in the lower right particle. In the upper left part, there is a mixed particle consisting of grains of martitic, granular, lamellar hematite and quartz. In the upper central particle, part of a particle is made up of several grains of quartz and hematite. Figure 5c shows the presence of free particles of very porous martitic hematite, quartz, amphibolitic and earthy goethite. At the bottom right, there is an aggregate of granular and lamellar hematite. Figure 5d shows the free quartz grains and the presence of martitic hematite in larger grains than the lamellar ones.

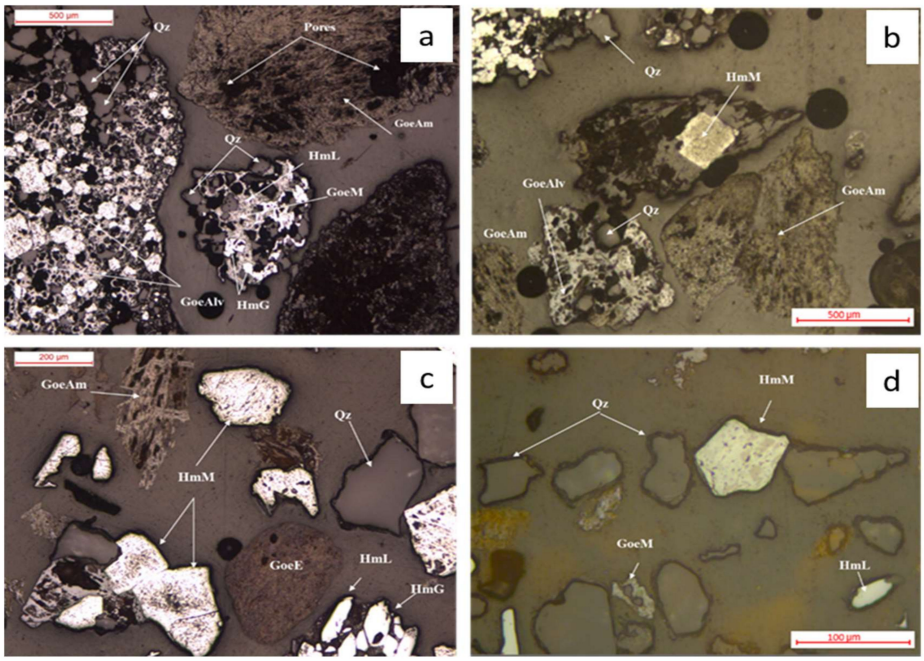

Figure 5. Reflected light optical microscopy images: (**a**) particle size fraction +1000 µm (parallel polarizers) showing the goethite: amphibolitic (GoeAm) porous, alveolar (GoeAlv) and massive (GoeM) with granular hematite (HmG) and lamellar (HmL, upper left particle); (**b**) particle size −1000 + 500 µm (parallel polarizers) containing martitic hematite (HmM, central grain), quartz (Qz), alveolar goethite (GoeAlv) and amphibolitic (GoeAm, lower right particle); (**c**) particle size fraction −500 + 150 µm (parallel polarizers) showing the presence of particles free of quartz (Qz), martitic hematite (HmM), amphibolitic goethite (GoeAm) and earthy goethite (GoeE), in addition to a particle containing lamellar (HmL) and granular (HmG) hematite grains, and (**d**) particle size −150 +45 µm (parallel polarizers) highlighting the presence of free quartz (Qz), martitic hematite (Hm), lamellar hematite (HmL) and massive goethite (GoeM).

Figure 6 shows photomicrographs of the SEM, showing the microtextures of the amphibolitic itabirite's goethite studied. On the left, (a) fibrous amphibolitic goethite, (b) massive goethite and (c) alveolar goethite [11,29]. Silva et al. [3], through detailed studies by optical microscopy and SEM/EDS, carried out with a sample of goethitic iron ore from Alegria, in the eastern region of Quadrilátero Ferrífero, verified the presence of the elements P, Al and Si in the chemical structure of goethite, highlighting the occurrence of isomorphic substitution of Fe for Al in the chemical structure of goethite. According to these authors, earthy goethite has higher grades of Al_2O_3, and massive goethite has higher grades of SiO_2.

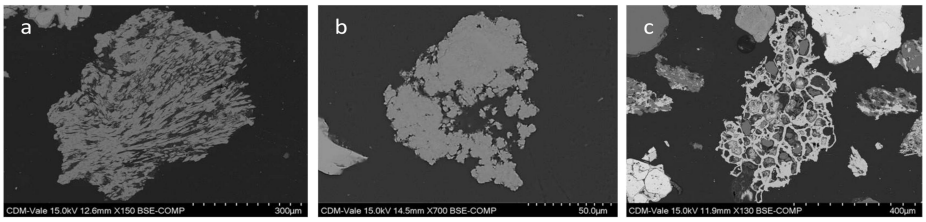

Figure 6. Backscattered electron images of the SEM, showing microtextures of goethite from the studied amphibolitic itabirite: (**a**) fibrous amphibolitic, (**b**) massive and (**c**) alveolar.

The quartz (main gangue mineral in the sample) liberation is shown in Figure 7. Based on the study of the quartz liberation, the ore was fragmented below 105 µm for the subsequent concentration tests.

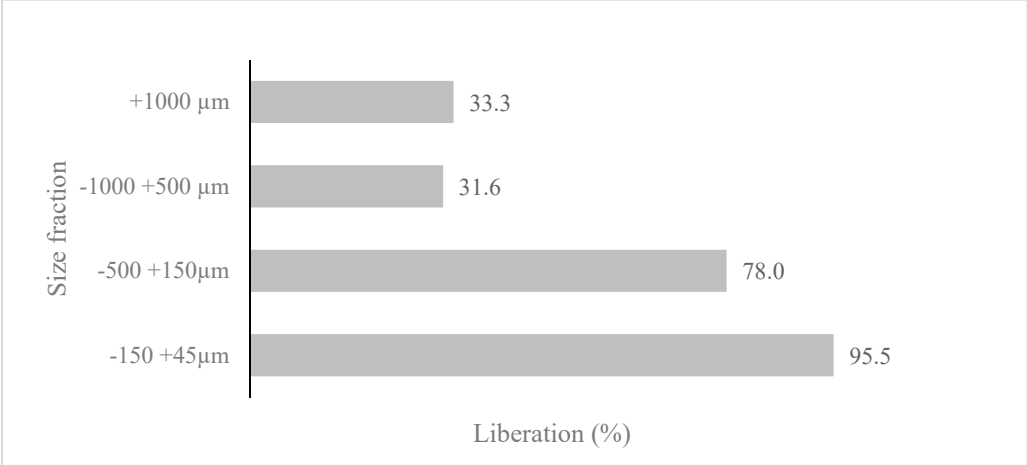

Figure 7. Quartz liberation in regard to the iron minerals of amphibolitic itabirite.

3.4. Proposal of the Beneficiation Route

Based on the physical, chemical and mineralogical characterization of the amphibolitic itabirite sample, concentration tests (magnetic and flotation) were carried out with the sample comminuted to −105 µm.

Table 4 presents the mass and metallurgical balances of the desliming operation. As can be seen, the Fe, Al_2O_3 and LOI grades in the slimes are higher than in the deslimed and non-deslimed samples. Probably, in this sample, there are higher proportions of goethite and gibbsite. The SiO_2 (quartz) in the deslimed sample is higher than in both slimes and non-deslimed samples. The grades of Al_2O_3, P and LOI are smaller in this sample compared with the non-deslimed (−105 µm) and slime samples. It means that these impurities are associated with particles −10 µm (slimes). In terms of distribution, about 38% of the value (Fe) can be discarded as slimes. The distribution of Al_2O_3 is higher in slimes due to a higher proportion of gibbsite in this sample.

Table 4. Mass and metallurgical balances of the desliming operation.

Sample	Weight (%)	Grade (wt%)						Distribution (%)					
		Fe	SiO_2	P	Al_2O_3	Mn	LOI	Fe	SiO_2	P	Al_2O_3	LOI
Deslimed (−105 µm)	66.9	43.1	33.0	0.100	0.56	0.128	5.03	62.3	84.2	49.2	41.1	51.1
Slimes	33.1	52.8	12.5	0.209	1.62	0.084	9.73	37.7	15.8	50.8	58.9	48.9
Non-deslimed (−105 µm)	100.0	46.0	25.5	0.137	0.95	0.156	6,69	100.0	100.0	100.0	100.0	100.0

As can be seen in Table 5, the Fe recoveries of the magnetic concentration tests, carried out with the non-deslimed sample, for both magnetic field intensities (0.9 and 1.1 T) were low and very similar (~27%). The grades of Fe and SiO_2 also were similar. San et al. [30], after the hydrophobic flocculation of limonite iron ore fines (~38 wt% Fe), increased the performance of magnetic separation for a magnetic field of 1 T: Fe recovery increased from 48.2% to 81.7%, with similar grades in the obtained concentrates (~51 wt% Fe). For Brazilian slimes with high contents of goethite (51.4 wt% Fe and 15.1 wt% SiO_2), after flocculation by starch followed by magnetic separation (magnetic field of 0.3575 T) was reached Fe recovery of 53.3% with concentrate grades of Fe and SiO_2 equal to 59.4 wt% and 7.4 wt%, respectively [7].

Table 5. Results of the concentration tests carried out with the non-deslimed and deslimed samples of amphibolitic itabirite (−105 μm).

Magnetic Concentration						
Sample	**Magnetic Field (T)**	**Pulp (wt%)**	**Mass Recovery (%)**	**Fe Recovery (%)**	**Concentrate Grade (%)**	
					Fe	**SiO_2**
Non-deslimed (−105 μm)	0.9	40	26.6	27.5	61.2	6.8
Non-deslimed (−105 μm)	1.1	30	20.0	26.7	60.7	6.9
Deslimed	0.9	-	67.0	92.61	59.0	7.9
Flotation (Deslimed Sample)						
Amine (g/ton)			**Mass Recovery (%)**	**Fe Recovery (%)**	**Concentrate Grade (%)**	
					Fe	**SiO_2**
170			36.7	53.9	61.7	2.2
200			34.8	50.0	62.7	1.8

For a 0.9 T magnetic field, the Fe recovery of the deslimed sample increased from ~27.1% to 92.6%, with a decrease of only 2% and 1% of the Fe and SiO_2 grades, respectively, in the obtained concentrate. The better performance of the magnetic concentration of the deslimed sample compared with the non-deslimed sample is related with the high content of slimes (−10 μm particles) in the non-deslimed sample (~33%) compared with deslimed sample (~10%). Therefore, as well-known previous desliming operation is essential for an efficient conventional magnetic separation. For reverse flotation (Table 5), both the Fe and SiO_2 grades in the obtained concentrates of the deslimed sample were similar for amine dosages of 170 and 200 g/ton. Compared with the magnetic concentrate of the same sample (0.9 T field magnetic), the Fe grade was about 3–4% smaller, and the SiO_2 grade was ~6% higher. however, both the mass recovery and Fe recovery were smaller by 32.2% and 42.6%, respectively, compared with the magnetic concentration. It means a huge loss of values for tailings. Although, both reverse flotation, using amine/starch, and magnetic concentration are recommended to concentrate iron ore, whose hematite or goethite are the main bearing minerals of iron, and quartz is the main gangue mineral, the performance of magnetic flotation was better compared with the flotation for the studied ore [31].

Figure 8 shows the proposed flowsheet (open circuit) for processing the sample studied for a 0.9 T magnetic field, where the mass balances and product grades obtained in each unit operation are presented.

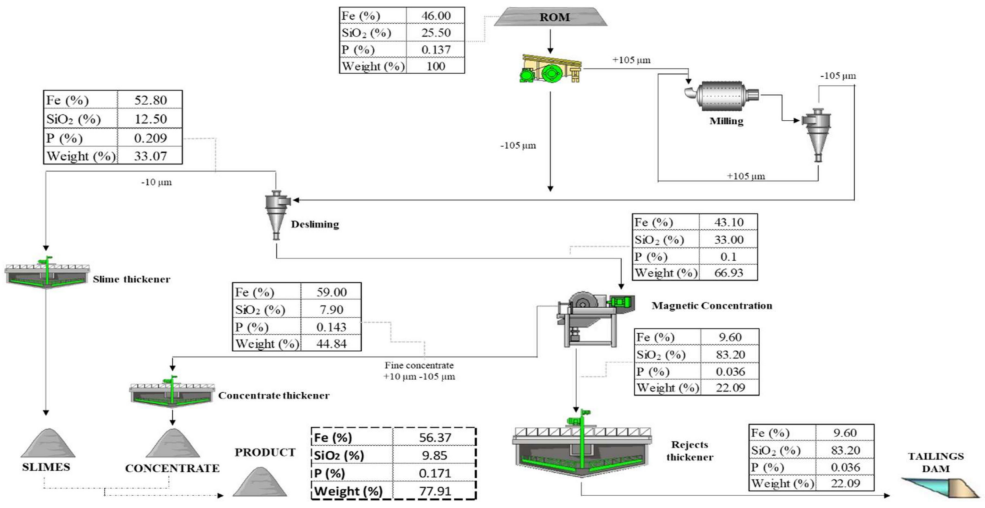

Figure 8. Proposed flowsheet of the magnetic concentration of the amphibolitic itabirite (open circuit).

It can be ascertained from Figure 8 that the slimes represent more than 30% of the feed, with a grade (52.8% Fe) much higher than the grade of the circuit's feed of 46% Fe. After the magnetic concentration of the deslimed ore (43% Fe), there is a 16% increase in the Fe grade in regard to the original sample. With the disposal of the slimes, the mass recovery of the circuit would be approximately 45%. The addition of slimes to the product of the magnetic concentration of the deslimed ore could be used as a poor "pellet feed", which can be blended with other products of higher grades in the pelletizing stage, greatly increasing the mass recovery and, consequently, reducing the discarded waste. Lima and Abreu [7] obtained, through selective flocculation/magnetic separation of a slimes sample from the Fundão/Samarco's tailings dam, with grades and a particle size distribution similar to the amphibolitic itabirite slimes, a concentrate with 59% Fe and a mass recovery of approximately 50% for the following conditions: pH = 10.5, sodium silicate and corn starch = 50 g/ton and magnetic field 0.3575 T. Therefore, the possibility of testing this concentration route for the slimes of the studied ore could be evaluated.

4. Conclusions

Studies of physical, chemical and mineralogical characterization carried out with the sample of amphibolitic itabirite from the eastern region of Quadrilátero Ferrífero showed that the natural moisture of the ore is 10%, and the specific weight is 3710 kg/m^3. These values are consistent with the mineralogical and microtextural compositions of the sample, which consist basically of 64.5% goethite (amphibolitic, alveolar, massive and earthy) and hematite (6.8%), mainly martitic, which are quite porous, and quartz (25.5%). For this reason, high proportions of slimes are generated in the comminution stage for the quartz liberation in 105 μm, which represent 33% of losses in the desliming stage, with Fe grades (~52%) higher than that of the ROM ore (46%) and deslimed ore (43%). Among the concentration tests (magnetic and flotation) performed with the studied sample, the magnetic concentration (0.9 T magnetic field) of the deslimed ore and subsequent blending of the concentrate obtained with the slimes provided a mass recovery of approximately 80% of the poor "pellet feed" to be added in the pelletizing process. however, further studies are needed to optimize the proposed circuit, in addition to the introduction of selective flocculation/magnetic separation of the generated slimes.

Author Contributions: Conception: G.M.C.G. and R.M.F.L.; methodology: G.M.C.G.; formal analysis: G.M.C.G. and R.M.F.L.; writing—original draft preparation: R.M.F.L. and G.M.C.G.; writing—review and editing: R.M.F.L. and G.M.C.G. All authors have read and agreed to the published version of the manuscript.

Funding: This research received no external funding.

Acknowledgments: The authors would like to thank Vale S.A. for the sample and use of its laboratory infrastructure, CNPq for the researcher grant to R.M.F.L., Capes and the Federal University of Ouro Preto.

Conflicts of Interest: The authors declare no conflict of interest.

References

1. Mohiuddin, K.; Strezovand, V.; Nelson, P.F. Industrial and environmental sustainability of ironmaking technologies. In *Advances in Environmental Research*; Daniels, J.A., Ed.; Nova Publishers: New York, NY, USA, 2011; Volume 12, pp. 131–152.
2. Serviço de Apoio às micro e Pequenas Empresas do Rio Grande do Norte. Boletim de Comércio Exterior Período 2012 a 2016. Natal. Available online: www.rn.sebrae.com.br/ (accessed on 20 July 2018).
3. Silva, M.S.S.; Lima, M.M.F.; Graça, L.M.; Lima, R.M.F. Bench-scale calcination and sintering of a goethite iron ore sample. *Int. J. miner. Process.* **2016**, *150*, 54–64. [CrossRef]
4. Veloso, C.H.; Filippov, L.O.; Filippova, I.V.; Araujo, A.C. Investigation of the interaction mechanism of depressants in the reverse cationic flotation of complex iron ores. *Miner. Eng.* **2018**, *125*, 133–139. [CrossRef]
5. USGS. Iron ore statistics and information. In *US Geological Survey Minerals Information*; US Department of Interior: Washington, DC, USA, 2020. Available online: https://pubs.usgs.gov/periodicals/mcs2020/mcs2020-iron-ore.pdf (accessed on 4 April 2020).

6. Dauce, P.D.; Castro, G.B.; Lima, M.M.F.; Lima, R.M.F. Characterisation and magnetic concentration of an iron ore tailings. *J. Mater. Res. Technol.-JMR&T* **2019**, *8*, 1052–1059.
7. Lima, R.M.F.; Abreu, F.P.V.F. Characterization and concentration by selective flocculation/magnetic separation of iron ore slimes from a dam of Quadrilátero Ferrífero/Brazil. *J. Mater. Res. Technol.-JMR&T* **2020**, *9*, 2021–2027.
8. Silva, M.B.; Luz, J.A.M. Magnetic scavenging of ultrafine hematite from itabirites. *Revista Escola de minas-REM* **2013**, *66*, 499–505. [CrossRef]
9. Sales, C.G. Rotas de Beneficiamento para Recuperação de minerais Portadores de Ferro do Underflow do Espessador de Lamas da Usina de Brucutu. Master's Thesis, Universidade Federal de minas Gerais—UFMG, Belo horizonte, Brazil, 2012.
10. Alkmim, F.F.; Amorim, L.Q. New ore types from the Cauê banded iron-formation. Quadrilátero Ferrífero. minas Gerais. Brazil—Responses to the growing demand. In Proceedings of the IRON ORE CONFERENCE, Perth, Australia, 11–13 July 2011; p. 13.
11. Rocha, J.M.P. Definição da Tipologia e Caracterização mineralógica e Microestrutural dos Itabiritos Anfibolíticos das minas de Alegria da Samarco mineração S.A.—Minas Gerais. Ph.D. Thesis, Universidade Federal de minas Gerais, UFMG, Belo horizonte, Brazil, 2008.
12. Roberto, J.B. Influência dos Diversos Tipos Litológicos nas Operações de Concentração da Instalação de Beneficiamento de Brucutu. Master's Thesis, Universidade Federal de minas Gerais, UFMG, Belo horizonte, Brazil, 2010.
13. Gonçalves, G.M.C. Caracterização Tecnológica do Itabirito Anfibolítico da mina de Brucutu-MG. Master's Thesis, Universidade Federal de Ouro Preto, UFOP, Ouro Preto, Brazil, 2020.
14. Lima, R.M.F.; Lopes, G.M.; Gontijo, C.F. Aspectos mineralógicos. físicos e químicos na flotação catiônica de minérios de ferro de baixos teores do Quadrilátero Ferrífero-MG. *Tecnol. em Metal. Mater. e mineração* **2011**, *8*, 126–131. [CrossRef]
15. Breuil, C.J.; Perroton, A.; Blancher, B.S.; Rodriguez, C.; Meschi-Daniel, A.F.; Wallmach, T. Iron oxides evolution along the lateritic profile of mabounié carbonatite (Gabon): A key point to understand magnetic separation processes. *Miner. Resour. Sustain. World* **2015**, *4*, 1369–1372.
16. Stradling, A.W. Development of a mathematical model of a crossbelt magnetic separator. *Miner. Eng.* **1991**, *4*, 733–745. [CrossRef]
17. Santos, P.A. Estudo de Densidade de Rochas e Comparação de Técnicas de Medição na Região do Quadrilátero Ferrífero. minas Gerais. Brasil. Bachelor's Thesis, Instituto Superior de Educação de Itabira—ISEI, Itabira, Brazil, 2006; p. 70.
18. Caldeira, E.; Angeli, G.; Cunha, E.; Roldão, D. Revisão de recursos da mina de Brucutu. *Relat. Interno Vale* **2011**, *1*, 43–45.
19. Freitas, L.S. Avaliação dos minérios Itabiritos Compactos e Semi-Compactos em um Circuito de Britagem da Samarco mineração S/A. Master's Thesis, Universidade Federal de minas Gerais—UFMG, Belo horizonte, Brazil, 2014.
20. Queiroz, L.A.; Brandão, P.R.G. Aspectos mineralógicos relacionados à concentração magnética de minério de ferro itabirítico. *Metal. Mater.* **2009**, *65*, 148–154.
21. Neumann, R.; Avelar, A.N.; da Costa, G.M. Refinement of the isomorphic substitutions in goethite and hematite by the Rietveld method, and relevance to bauxite characterisation and processing. *Miner. Eng.* **2014**, *55*, 80–86. [CrossRef]
22. Liu, H.; Chen, T.; Xie, Q.; Zou, X.; Qing, C.; Frost, R. Kinetic study of goethite dehydration and the effect of aluminium substitution on the dehydrate. *Thermochim. Acta* **2012**, *545*, 20–25. [CrossRef]
23. Liu, H.; Chen, T.; Chang, J.; Zou, X.; Frost, R. The effect of hydroxyl groups and surface area of hematite derived from annealing goethite for phosphate removal. *J. Colloid Interface Sci.* **2013**, *398*, 88–94. [CrossRef] [PubMed]
24. Liu, H.; Chen, T.; Zou, X.; Qing, C.; Frost, R. Thermal treatment of natural goethite: Thermal transformation and physical properties. *Thermochim. Acta* **2013**, *568*, 115–121. [CrossRef]
25. Costa, G.M.; Novack, K.M.; Elias, M.M.; Cunha, C.R.F. Quantification of moisture contents in iron and manganese ores. *ISIJ Int.* **2013**, *53*, 1732–1738. [CrossRef]
26. Weissenborn, P.K.; Dunn, J.G.; Warren, L.J. Quantitative thermogravimetric analysis of haematite. goethite and kaolinite in western Australian iron ores. *Thermochim. Acta* **1994**, *239*, 147–156. [CrossRef]
27. Schwertmann, U. The double dehydroxylation peak of goethite. *Thermochim. Acta* **1984**, *78*, 39–46. [CrossRef]

28. MacKenzie, K.J.D.; Temuujin, J.; Okada, K. Thermal decomposition of mechanically activated gibbsite. *Thermochim. Acta* **1999**, *327*, 103–108. [CrossRef]
29. Magalhães, M.S.; Brandão, P.R.; Tavares, R.P. Types of goethite from Quadrilátero Ferrifero's iron ores and their implications in the sintering process. *Trans. Inst. min. Metall.* **2007**, *116*, 54–64. [CrossRef]
30. Song, S.; Lu, S.; Lopez-Valdivieso, A. Magnetic separation of hematite and limonite fines as hydrophobic flocs from iron ores. *Miner. Eng.* **2002**, *15*, 415–422. [CrossRef]
31. Araujo, A.C.; Amarante, S.C.; Souza, C.C.; Silva, R.R.R. Ore mineralogy and its relevance for selection of concentration methods in processing of Brazilian iron ores. *Miner Process. Extr. Metall.* **2003**, *112*, C54–C64. [CrossRef]